Theor Chem Acc (2007) 117: 267–273
DOI 10.1007/s00214-006-0141-1

REGULAR ARTICLE

Ansuman Lahiri · Joanna Sarzynska
Lennart Nilsson · Tadeusz Kulinski

Molecular dynamics simulation of the preferred conformations of 2-thiouridine in aqueous solution

Received: 30 June 2005 / Accepted: 30 November 2005 / Published online: 5 July 2006

Abstract Transfer RNA (tRNA) molecules display a large diversity of posttranscriptionally modified nucleosides at the anticodon wobble at position 34 and 3′ to the anticodon triplet at position 37. Some of these modifications appear to play an important role in the recognition of the correct codon on the ribosome. It has been suggested that these modifications work by regulating the conformational rigidity/flexibility of the nucleosides at those positions. We present here the results of a molecular dynamics study where we compare the conformational characteristics of uridine and 2-thiouridine in aqueous solution. We find that a newly derived parameter set for thio-modified uridines for the CHARMM27 force field for nucleic acids correctly reproduces the experimental observations. We also found that replica exchange molecular dynamics method with generalized Born molecular volume implicit solvent approximation reproduces the experimental observations at a much less computational effort and therefore may be considered as a promising method for simulating larger systems such as ribosome.

Keywords Codon-anticodon interaction · Replica exchange molecular dynamics · Implicit solvent model · Generalized Born molecular volume

Ansuman Lahiri and Joanna Sarzynska have contributed equally to this paper.

A. Lahiri (✉)
Department of Biophysics, Molecular Biology and Genetics, University of Calcutta, 92, APC Road, Kolkata 700009, India
E-mail: albmbg@caluniv.ac.in

J. Sarzynska · T. Kulinski
Institute of Bioorganic Chemistry, Polish Academy of Sciences, Noskowskiego 12/14, 61 704 Poznan, Poland

L. Nilsson
Center for Structural Biochemistry, Department of Biosciences, Karolinska Institutet, 141 57 Huddinge, Sweden

1 Introduction

A crucial step in the initial stage of ribosomal protein synthesis is the correct recognition of the codon on the mRNA by the corresponding cognate anticodon of the tRNA. The aminoacyl-tRNA binds to the A-site of the ribosome in a ternary complex with elongation factor Tu and GTP and after a preliminary selection of codon–anticodon matching, a complicated set of conformational changes and GTP hydrolysis takes place in the complex resulting in the rejection of an incorrect codon–anticodon match [1].

An intriguing point in this issue is that posttranscriptional modification of bases in the first position of the anticodon of the tRNA (the so-called wobble position) is very common as is also modification of the base 3′ to the anticodon. These modifications have important functional roles in that they have been shown to affect ribosome binding [2–4], missense error rates [5], frameshifting frequency [6], speed of translation [7] and initiation of HIV-1 reverse transcription [8,9].

It is quite likely that these functional roles originate from structural differences caused by the modifications. NMR studies have indeed found evidences that tRNA anticodon sequences that are natively modified lose the canonical loop structure of the anticodon if they are replaced by unmodified bases and the canonical loop structure can be remodeled by reintroduction of base modifications [10–12].

2-thiouridine (s^2U) is a relatively simple base modification that demonstrates distinct functional effect in ribosome binding and codon recognition on the ribosome [2–4]. NMR investigations on the nucleoside in solution have shown that s^2U is conformationally more rigid compared to unmodified uridine (U) [13,14].

In a recent study [15] extensive molecular dynamics simulations of the eight standard nucleosides were performed in explicit solvent to obtain equilibrium populations of the torsion angles, their kinetics of interconversion, their coupling and the way they are affected by water. Such a full characterization is not available from experimental approaches and the simulation results were found to corroborate and complement experimental observations.

Of the many possible extensions of this study, we wish to highlight two directions. Firstly, such extensive conformational characterization is unavailable for the nonstandard or modified nucleosides. In many cases, there are no parameters for the modified bases. Secondly, it was observed that to obtain reliable conformational distribution in explicit solvent, very long simulations are necessary. For the case of the eight nucleosides, the simulations were of 50 ns length. It is necessary to extend the force field to include biologically important modified bases and also to devise more efficient ways of sampling their conformational characteristics to be able to treat realistic system sizes in the near future.

With a long-term aim to gain detailed understanding of the problem of the dynamics of anticodon–codon recognition on the ribosome and the role of modified bases in it by using molecular dynamics simulations, we have chosen to study conformational characteristics of s^2U with a twofold objective. Our first objective is a functional validation of the new parameter set for the modified RNA base 2-thiouridine derived for the extensively used CHARMM27 force field for nucleic acids [16] that has been quite successful in modeling and simulation of nucleic acid properties in explicit solvent. The second objective is to test for this simple model system whether a faster and much more computationally efficient simulation protocol, the replica exchange molecular dynamics (REMD) method [17] under the generalized Born molecular volume (GBMV) [18,19] implicit solvent approximation, yields equivalent results. The latter test is crucially important for the reason that simulation of anticodon–codon recognition in situ in ribosome will be computationally much more tractable if enhanced sampling methods coupled with implicit solvent approximations are applicable.

2 Computational details

All molecular mechanics and dynamics calculations were performed with the program CHARMM [20] versions 30 and 31 using the CHARMM27 nucleic acid force field [16].

2.1 Parameter set for 2-thiouridine

Parameterization of s^2U was performed according to parameterization philosophy of the CHARMM27 nucleic acid force field [16,21]. Parameters for the sugar are the same as for the ribose in CHARMM27. The topology and parameters for 2-thiouracil together with parameters for 4-thiouracil compatible to the CHARMM27 force field were developed by us recently [22] and are briefly described here for completeness.

The initial topology information (connectivity, atom types), and as a consequence most internal parameters for 2-thiouracil were transferred directly from uracil. For sulphur, the atomic type found in methanethiol in the CHARMM22 protein all-hydrogen parameters was taken, which simultaneously assigned its van der Waals (VDW) parameters. Missing internal parameters, unique to the new base, were only bond, angle and torsion parameters associated with the sulphur atom. These parameters were assigned by analogy to existing parameters. The partial atomic charges were adjusted to get the best agreement between the energies and the distances obtained from CHARMM and quantum mechanical (QM) calculations for individual water molecules interacting with different sites on 2-thiouracil. The QM minimum interaction energies and distances between different sites of the studied bases and individual water molecules placed in idealized orientations were determined at the HF/6-31G* level by optimizing the interaction distances. The molecular mechanics minimum interaction energies and distances between bases and water molecules were determined in CHARMM by varying the interaction distances. The orientations of the individual water molecules were identical to those used in the QM calculations. The CHARMM calculations were performed with no truncation of nonbonded interactions and the dielectric constant $\varepsilon = 1$. The TIP3P model [23] for water was used in QM and CHARMM calculations.

The bond and angle equilibration values for newly introduced parameters were manually adjusted to better reproduce the geometry extracted from the crystal structure of 2-thiouracil [24].

2.2 Molecular dynamics

Initial nucleoside structures for molecular dynamics (MD) were built in a C3′-endo, *anti* conformation and energy minimized in vacuum gently. Each nucleoside was solvated in a $30 \times 30 \times 30\,\text{Å}^3$ box of preequilibrated TIP3P water. Water molecules closer than 2 Å from any nucleoside atom were removed. The whole system contained 2,690 (including 887 water molecules) and 2,696 atoms (including 889 water molecules) for uridine and s^2U simulation, respectively. The water was then subjected to 10 ps of MD keeping the nucleoside fixed. The system was heated from 50 to 300 K in 12 ps in 50 K increments. The MD simulations were performed in constant volume and the temperature was periodically checked and kept within the window 300 ± 10 K. Simulations were run with periodic boundary conditions (PBC). The particle mesh Ewald (PME) method was used for treatment of electrostatic interactions [25]. A real space cutoff was set to 12 Å, the number of grid points was set to 64 in each direction and the screening parameter (κ) to 0.32. Van der Waals interactions were truncated at 12 Å with a switching function from 10 to 12 Å. The nonbonded atom pair list was generated using a 14 Å cutoff and updated when any atom had moved 1 Å or more. MD simulations were run with a 2 fs time step and SHAKE algorithm [26] to constrain all bonds to hydrogens. Coordinates were saved for analysis every 1 ps. The first 1 ns was excluded from the analysis.

2.3 Replica exchange molecular dynamics

Replica exchange molecular dynamics (REMD) calculations were carried out using the multiscale modeling tools for

structural biology (MMTSB) interface [27] to CHARMM. In replica exchange method [17] several simulations or replicas of the same system are run at different temperatures, using separate processors. Temperatures are exchanged between two replicas, i and j, with the probability $P(\text{exchange}) = \exp-(\beta_i - \beta_j)(E_i - E_i)$, where $\beta = 1/k_B T$, k_B is the Boltzmann constant, T is the absolute temperature, and E is the potential energy. In this study we ran REMD both in explicit water and in implicit solvent using the generalized Born molecular volume implicit solvent approximation [18,19].

The simulation system for REMD in explicit water was the same as for standard MD. As the initial structure for REMD we took the conformation after 500ps of standard MD. Sixteen temperatures were used: T = 300.0, 305.8, 311.7, 317.8, 323.9, 330.2, 336.6, 343.1, 349.7, 356.5, 363.4, 370.5, 377.6, 384.9, 392.4 and 400.0 K. After 50 ps of equilibration at target temperatures replicas attempted exchange. The simulations were carried out for 2,000 cycles consisting of 500 steps of MD (1 ps), giving 2 ns for each replica and a total of 32 ns of simulation time. The acceptance ratio of exchange between temperatures ranged between 28 and 39%.

For REMD with implicit solvent we simulated eight replicas running at temperatures 298, 310.8, 324.1, 338.1, 352.6, 367.7, 383.5 and 400 K. The REMD cycles consisted of 200 steps of molecular dynamics (0.4 ps) followed by attempted exchange between replicas with neighboring temperatures. After 40 ps of equilibration at target temperatures, 2 ns per replica of production runs were collected for each nucleoside. The acceptance ratio was about 80%.

The Nosé–Hoover algorithm [28,29] was used for temperature control within each trajectory with a coupling constant of 50 and the velocity Verlet integrator [30] was used with a time step of 2 fs with all bonds involving hydrogen atoms constrained by SHAKE [26]. Nonbonded interactions were calculated without cutoffs. The solvent electrostatic contribution was modeled by the GBMV method implemented within CHARMM [19] using a solvent dielectric constant of 80. The GBMV model is based on the generalized Born equation which provides an approximation to the electrostatic screening interaction between two charged groups in the presence of a continuum dielectric. The total solvation free energy can be written as [31]

$$\Delta G^{\text{solvation}} = \sum_i \left(\Delta E_i^{\text{self}} - \frac{1}{2} \sum_{j \neq i} E_{ij}^{\text{screen}} + \Delta E_i^{\text{nonpolar}} \right)$$

The first term within the parentheses can be calculated using an approximation to the integral of the energy density of the electric field over space. In the GBMV approach, the screening term is approximated rather accurately by employing an empirical correction term for the effective Born radii. The nonpolar solvation term is taken to be proportional to molecular solvent-accessible surface area (SASA), and the GBMV hydrophobic SASA term factor was set to 0.005.

2.4 Structural analysis

We follow the convention of Saenger [32] in the atom names and dihedral angle nomenclature. The magnitude of sugar puckering pseudorotation angles (P) were calculated following Altona and Sundaralingam [33]. For convenience in comparison with NMR studies, we have adopted a two-state model for the pseudorotation angle, in which the pseudorotation space is divided into NORTH ($270° \leq P < 90°$) and SOUTH ($90° \leq P < 270°$) partitions.

The *anti* conformations of the torsion angle χ measured with respect to O4′-C1′-N1-C2 are defined as the 170–300° range and the *syn* conformation is defined as 30–90° range. The values of χ falling outside are referred to as other.

Torsion γ is measured with respect to O5′-C5′-C4′-C3′ and classified as $g^+(60 \pm 30°)$, $g^-(-60 \pm 30°)$, and trans (180 ± 30^o). The values of γ that fall outside these ranges are referred to as other.

3 Results and discussion

The main result of this work is summarized in Table 1 where we compare the experimental data from NMR studies [13,14, 34] for the equilibrium distribution of NORTH and SOUTH form of sugar pucker in the nucleosides uridine and 2-thiouridine with the distributions obtained from molecular dynamics simulations. We have also included in the table the results of the 50-ns-long molecular dynamics simulation of uridine in explicit solvent as reported in [15] for comparison.

The experimentally obtained pucker distribution for uridine is found to be strikingly similar among experiments and the NORTH and SOUTH conformations are found to be almost equally populated with a somewhat larger preference for the NORTH conformation. The two experiments [13,14] that report measurement of pucker distribution for s^2U convincingly show the dominance of the NORTH conformation over the SOUTH.

Molecular dynamics simulation in explicit solvent yields almost identical distribution for the pseudorotation angle for uridine in our work as well as in the result reported in [15]. However, in comparison with the distributions reported in the NMR investigations [13,14,34], the simulations in explicit solvent appear to overestimate the preference for the NORTH conformation (Fig. 1a).

Our explicit solvent simulation also somewhat overestimates the distribution of the pseudorotation angle for s^2U compared to experiment [14]. The fluctuation time series of the pseudorotation angle for both nucleosides in Fig. 2 shows that for a time period of over 30 ns uridine interconverts between the NORTH and SOUTH forms much more frequently than s^2U. The relative motional rigidity of s^2U might be a reason for our observation that for a shorter time scales of simulation ($\sim$ 2 ns) the distribution of pseudorotation angle appeared just the opposite of what one obtains at longer time scales. This also confirms that long simulations are necessary

Table 1 The equilibrium distributions (%) of NORTH and SOUTH conformations of uridine and 2-thiouridine

Nucleoside	U		s^2U	
	NORTH	SOUTH	NORTH	SOUTH
NMR [32]	54	46		
NMR[a] [13]	55	45	74	26
NMR[b] [14]	53	47	71	29
MD [15]	72	28		
MD[c]	70	30	83	17
REMD[c,d]	73	27	77	23
REMD[c,e]	54	46	89	11

[a]Calculated from ΔG according to the equation $\%S(T) = 100[\exp(-\Delta G/RT)]/[\exp(-\Delta G/RT) + 1]$
[b]Calculated from coupling constants ($J_{1'2'}/J_{3'4'}$) by formulas $\%S = 100[J_{1'2'}/(J_{1'2'} + J_{3'4'})]$, $\%N = 100[J_{3'4'}/(J_{1'2'} + J_{3'4'})]$
[c]This work
[d]Explicit solvent model, results are shown at T = 300 K
[e]Implicit solvent model, results are shown at T = 298 K

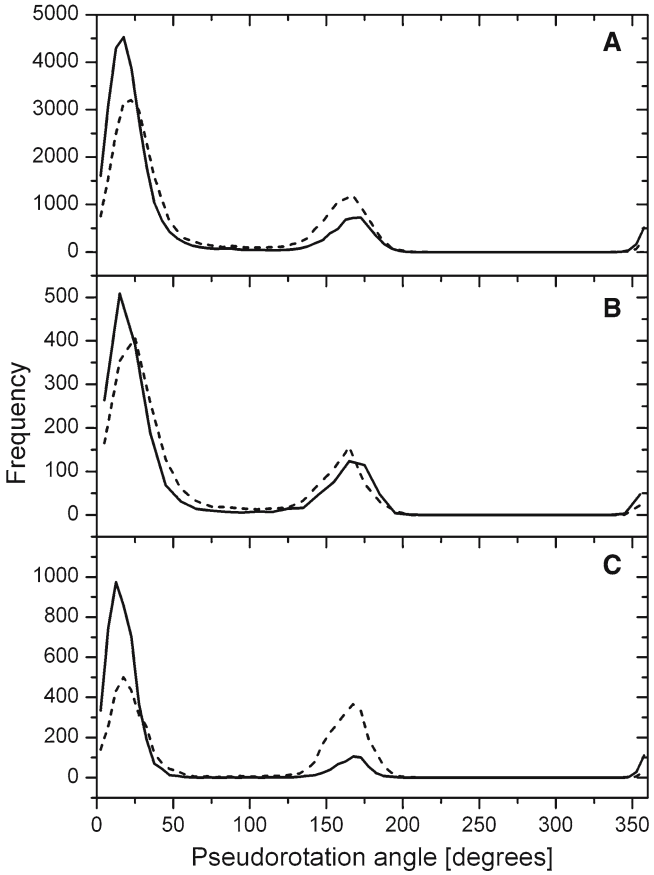

Fig. 1 Distribution of the pseudorotation angle (P) of s^2U (*solid line*) and uridine (*dashed line*); **a** from molecular dynamics simulation in explicit solvent, **b** from REMD in explicit solvent, **c** from REMD using the generalized Born molecular volume implicit solvent approximation

to arrive at reliable distributions for conformational degrees of freedom for even such a small system as a nucleoside [15].

The REMD approach has been successful in overcoming the problem of adequate sampling by running several simulations of the same system at different temperatures but periodically, at short time intervals, the individual simulations are coupled through a Monte Carlo based exchange of temperatures.

The distribution of sugar conformers for s^2U obtained from REMD in explicit water fell between results obtained from NMR and standard MD (Fig. 1b). The distribution of conformers for uridine under the same simulation conditions was very similar to the results obtained from both of the explicit solvent molecular dynamics simulations.

There is already a large number of simulation results involving REMD of biomolecules in implicit solvent which intend to couple the enhanced sampling ability of REMD with the computational efficiency of implicit solvent models. Ohkubo and Brooks [35] used the generalized Born/surface area (GB/SA) method to calculate the variation of conformational entropy with chain length for model peptides. Peptide folding was also simulated with a similar approach [36,37]. In some cases, however, discrepancies between experimental observations and implicit solvent results were noted [38,39].

As can be seen from Table 1 and Fig. 1c, the REMD results in implicit solvent are consistent with the experimental results. There is excellent agreement with the experimental distribution of NORTH and SOUTH pucker conformations for uridine while for s^2U the preference for the NORTH form is somewhat overestimated.

The distribution of torsion angle χ in our simulations (Fig. 3) fell almost exclusively within the range of the *anti* conformation. The χ distribution for uridine is broader than that for s^2U, both in explicit and implicit solvent model, again confirming the dynamical rigidity of the modified nucleoside.

For the torsion angle γ the distributions are very similar for both the nucleosides and predominantly confined to the g^+ region of the conformational space (Fig. 4). Altogether, our simulations nicely corroborate the experimental observation that the preferred conformation of s^2U in aqueous solution is C(3′)-endo, *anti* and g^+ [14].

Using the distributions obtained from the MD simulations we determined the potential of mean force ($w(P)$) for pseudorotation interconversion according to the equation: $w(P) = -k_BT \ln\{\rho(P)\}$, where $\rho(P)$ is the probability distribution of the pseudorotation angle P (Fig. 5).

The free energy difference (ΔG) between NORTH and SOUTH forms is 0.5 kcal/mol and 0.95 kcal/mol for uridine and s^2U respectively (from the overall populations in Table 1), which for s^2U is in agreement with experimental data (1.0 kcal/mol) obtained from the temperature dependence of the equilibrium constants for the ribose ring puckering [32]. The calculated ΔG for uridine is larger than experimental value (0.1 kcal/mol). The energy barrier for the transition from the NORTH to the SOUTH conformation is 2.9 kcal/mol for s^2U and 2.1 kcal/mol for uridine.

It is now well established that a change in the electronic character of the nucleic acid bases modulates the conformations of the sugar moiety by the tunable interplay of stereoelectronic anomeric and gauche effects [40]. Strengthening of the anomeric effect by the nucleic acid base drives the

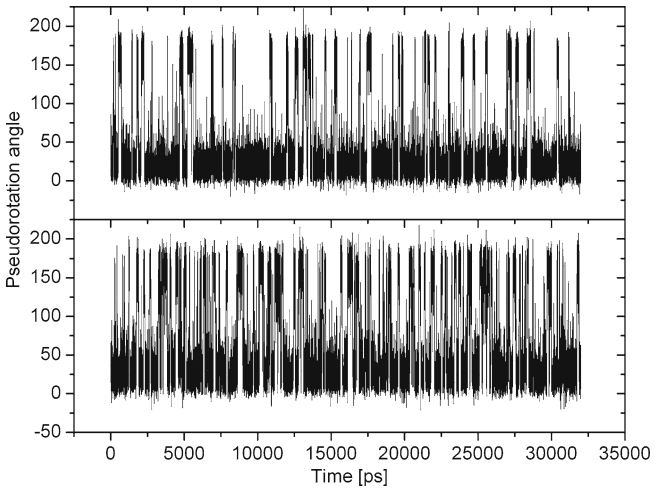

Fig. 2 Fluctuation time series of the pseudorotation angle showing transitions between NORTH and SOUTH conformations for s^2U (*upper panel*) and uridine (*lower panel*) obtained from molecular dynamics simulation in explicit solvent. The frequency of transitions is appreciably lower in the case of s^2U

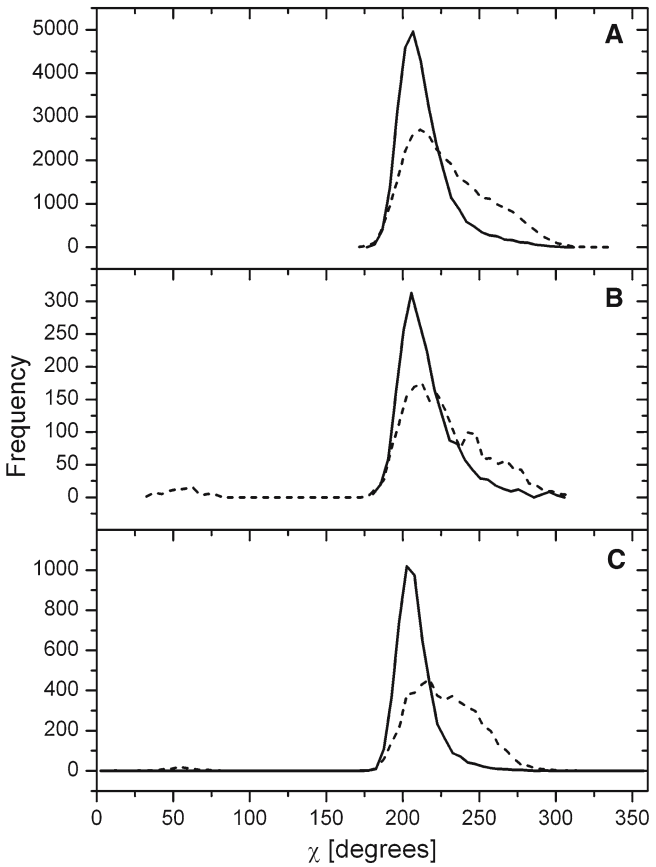

Fig. 3 Distribution of the torsion angle χ of s^2U (*solid line*) and uridine (*dashed line*); **a** from explicit solvent molecular dynamics simulation, **b** from REMD simulation in explicit solvent, **c** from REMD simulation in implicit solvent

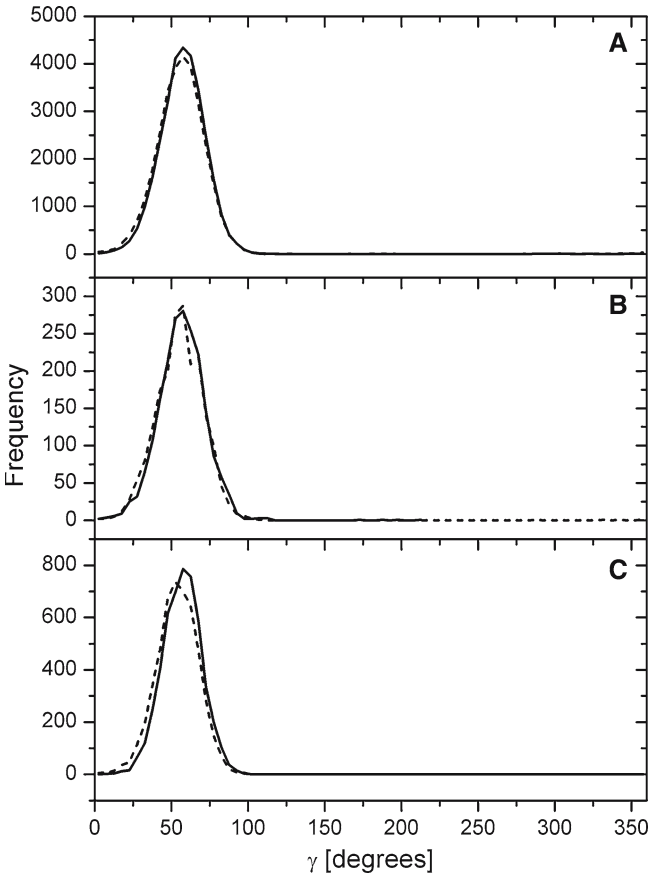

Fig. 4 Distribution of the torsion angle γ of s^2U (*solid line*) and uridine (*dashed line*); **a** from explicit solvent molecular dynamics simulation, **b** from REMD simulation in explicit solvent, **c** from REMD simulation in implicit solvent

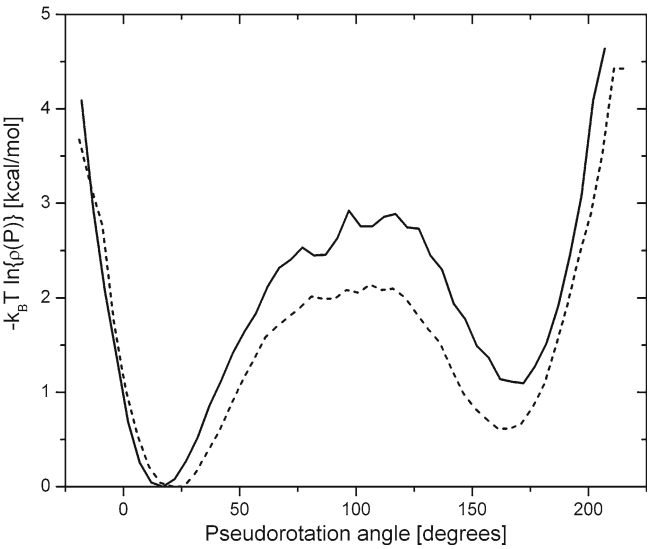

Fig. 5 Free energy projections along the pseudorotation angle for s^2U (*solid line*) and uridine (*dashed line*) computed from standard MD trajectories

sugar conformation towards the NORTH type conformers, the strength of these forces being dependent on the proper overlap between donor and acceptor orbitals.

In the present work, the stabilization of the NORTH conformation in s^2U is reproduced through classical interactions which have been calibrated against quantum calculations. Notably, in accordance with the philosophy of the development of CHARMM27 force field for nucleic acids, the sugar parameters for both the nucleosides have been kept identical. Even for the bases – bond, angle and torsion parameters not connected with the sulphur atom remained the same. The major difference in the parameter set came through the partial charges. Although the differences in the partial charges in the corresponding atoms in the bases were not directly related to the differences in the electron density distribution, but to a rather complicated procedure of fitting classical to quantum interaction energies with water, it is an interesting possibility that the partial charges so derived reflect the overall stereoelectronic effect. This is another issue that merits further study.

4 Conclusion

In the present work, we simulated the equilibrium conformational distribution of the nucleosides uridine and 2-thiouridine in aqueous solution by molecular dynamics and replica exchange molecular dynamics methods. Our objective was to obtain a functional validation of the new parameter set for the modified RNA base 2-thiouridine that has been derived for the extensively used CHARMM27 force field for nucleic acids. The second objective was to test whether a faster and much more computationally efficient simulation protocol, the replica exchange molecular dynamics method under the generalized Born molecular volume implicit solvent approximation, is a suitable approximation – at least for this model system.

We found good agreement between the simulated distributions and the experimental distributions of the nucleoside conformations confirming that a single thio-substitution at the carbon-2 position in uracil is sufficient to impart a considerable amount of conformational rigidity to the ribonucleoside so that the C(3′)-endo conformation becomes the dominant one. Our results using standard MD in explicit solvent and the PME method for long-range electrostatics are virtually identical to previous results [15] for uridine using a spherical cutoff that smoothly shifts energies and forces to zero at the cutoff distance 12 Å.

We also found the GBMV approximation to give similar distributions to the other methods. Coupled with REMD method it obtained the required distribution at a considerably less computational effort than normal MD with explicit solvent. From the foregoing, this approach may be considered as a powerful and promising method to simulate larger and complex systems such as ribosomes or its parts.

Acknowledgements This work was supported in part by grant from the State Committee for Scientific Research, Republic of Poland (4 T11F 010 24). The generous computational support of the Poznań Supercomputing and Networking Center is acknowledged.

References

1. Wintermeyer W, Peske F, Beringer M, Gromadski KB, Savelsbergh A, Rodnina MV (2004) Biochem Soc Trans 32:733
2. Ashraf S, Sochachka E, Cain R, Guenther R, Malkiewicz A, Agris P (1999) RNA 5:188
3. Yarian C, Marszalek M, Sochachka E, Malkiewicz A, Guenther R, Miskiewicz A, Agris PF (2000) Biochemistry 39:13390
4. Yarian C, Townsend H, Cszestkowski W, Sochachka E, Malkiewicz AJ, Guenther R, Miskiewicz A, Agris PF (2002) J Biol Chem 277:16391
5. Hagervall TG, Pomerantz SC, McCloskey JA (1998) J Mol Biol 284:33
6. Brierley I, Meredith MR, Bloys AJ, Hagervall TG (1997) J Mol Biol 270:360
7. Kruger M, Pedersen S, Hagervall T (1998) J Mol Biol 284:621
8. Isel C, Lanchy J-M, Le Grice SFJ, Ehresmann C, Ehresmann B, Marquet R (1996) EMBO J 15:917
9. Isel C, Marquet R, Keith G, Ehresmann C, Ehresmann B (1993) J Biol Chem 268:25269
10. Durant PC, Davis DR (1999) J Mol Biol 285:115
11. Sundaram M, Durant PC, Davis DR (2000) Biochemistry 39:12575
12. Durant PC, Bajji AC, Sundaram M, Kumar RK, Davis DR (2005) Biochemistry 44:8078
13. Yokoyama S, Watanabe T, Murao K, Ishikura H, Yamaizumi Z, Nishimura S, Miyazawa T (1985) Proc Natl Acad Sci USA 82:4905
14. Agris PF, Sierzputowska-Gracz H, Smith W, Malkiewicz A, Sochachka E, Nawrot B (1992) J Am Chem Soc 114:2652
15. Foloppe N, Nilsson L (2005) J Phys Chem B 109:9119
16. Foloppe N, MacKerell A (2000) J Comput Chem 21:86
17. Sugita Y, Okamoto Y (1999) Chem Phys Lett 314:141
18. Lee MS, Salsbury FR. Jr, Brooks CL III (2002) J Chem Phys 116:10606
19. Lee MS, Feig M, Salsbury FR. Jr, Brooks CL III (2003) J Comput Chem 24:1348
20. Brooks BR, Bruccoleri RE, Olafson BD, States DJ, Swaminathan S, Karplus M (1983) J Comput Chem 4:187
21. MacKerell AD (2001) In: Becker OM, MacKerell AD, Roux B, Watanabe M (eds) Computational biochemistry and biophysics, Marcel Dekker, Inc. New york, p 7
22. Sarzynska J, Kulinski T (2005) Comp Meth Sci Tech 11:49
23. Jorgensen WL, Chandrasekhar J, Madura J, Impey RW, Klein ML (1983) J Chem Phys 79:926
24. Tiekink ERT (1989) Zeitschrift Kristall 187:79
25. Darden T, York D, Pedersen L (1993) J Chem Phys 98:10089
26. Ryckaert J-P, Ciccotti G, Berendsen HJC (1977) J Comp Phys 23:327
27. Feig M, Karanicolas J, Brooks CL III (2004) J Mol Graph Model 22:377
28. Nose S (1984) Mol Phys 52:255
29. Hoover WG (1985) Phys Rev A 31:1695
30. Frenkel D, Smit B (1996) Understanding molecular simulation. Academic Press, San Diego
31. Jaramillo A, Wodak SJ (2005) Biophys J 88:156
32. Saenger W (1984) Principles of nucleic acid structure. Springer, Berlin Heidelberg, New York
33. Altona C, Sundaralingam M (1972) J Am Chem Soc 94:8205
34. Plavec J, Thibaudeau C, Chattopadhyaya J (1996) Pure Appl Chem 68:2137
35. Ohkubo YZ, Brooks CL III (2003) Proc Natl Acad Sci USA 100:13916

36. Pitera JW, Swope W (2003) Proc Natl Acad Sci USA 100:7587
37. Rhee MH, Pande VS (2003) Biophys J 84:775
38. Zhou RH, Berne BJ (2002) Proc Natl Acad Sci USA 99:12777
39. Nymeyer H, Garcia AE (2003) Proc Natl Acad Sci USA 100:13934
40. Acharya P (2003) Studies on the non-covalent interactions (stereo-electronics, stacking and hydrogen bonding) in the self-assembly of DNA and RNA. Ph.D. Thesis, Uppsala University